Uncertainties in coaxial cable transfer impedance

0. Abstract

The Electro-Magnetic Compatibility (EMC) design of aircraft and spacecraft has to consider the shielding effectiveness of metal braids around wires and cable bundles. The EMC design is usually supported by modelling and measurement of the transfer impedance of representative samples of metal braids. In practice it turns out that results of modelling tools and measurements are not always in good agreement, in particular for the higher frequencies in the MHz region. It appears that both modelling tools and measurement methods are subject to uncertainties. The objective of the present paper is to investigate these uncertainties. Therefore, a sensitivity analysis is applied to an analytical transfer impedance model. Results indicate that the determination of the average height between the carriers of a braided shield is a critical quantity to obtain accurate transfer-impedance predictions at high frequencies. Moreover, a multi-conductor transmission line (MTL) model for the line injection method as set-up for transfer impedance measurements is presented. This MTL model is used to analyse the sensitivity of termination loads and permittivities, and to show the differences in resonance effects on transfer impedance measurements caused by impedance mismatches and by differences in propagation speeds inside and outside the coax under test. Finally, uncertainties in the measurement set-up are discussed.

1. Introduction

In aerospace structures of aircraft and spacecraft a large number of avionic systems needs to be installed which requires routing of many wires and cables. Electrical currents in wiring induce electric and magnetic fields, which can cause electromagnetic interference, and degrade the performance of avionic systems installed in aircraft and spacecraft. Furthermore, there are environmental threats such as High Intensity Radiated Fields (HIRF), lightning and solar irradiance, which can disturb the transmission of signals. In order to ensure the desired reception and transmission of signals, wires and cables need to be shielded by metal braids. However, such shielding will certainly increase the weight and costs of aerospace structures. Therefore, the Electro-Magnetic Compatibility (EMC) design of aircraft and spacecraft has to consider the shielding effectiveness of metal braids in relation to the weight of the braids.

The shielding effectiveness of braids is governed by the transfer impedance Z_t of shields:

$$Z_t = \frac{1}{I_o}\frac{\partial V}{\partial z}, \tag{1}$$

where I_0 is the current flowing through the shield induced on its outer surface and $\partial V/\partial z$ is the voltage per unit length on the inside of the shield. This concept was initially introduced by Schelkunoff [1]. The transfer impedance is an intrinsic parameter whose value depends only on the geometry and materials of the braid. It allows estimating the electromagnetic effect in the wires inside the cable produced by an external field or, reciprocally, the radiation leaked from inside the cable to the environment. A low Z_t indicates few coupling between interior and exterior of the shield, and therefore a good shielding against interfering electromagnetic fields.

For the design of metal braids many analytical models are available: Vance [2], [3], Tyni [4], Kley [5] and Katakis [6]. These analytical models contain in general two components: a first part (Z_d) representing diffusion of electromagnetic energy through the metal braid, and a second part ($j\omega M$) representing leakage of magnetic fields through the braid:

$$Z_t = Z_d + j\omega\upsilon M. \tag{2}$$

Here υ is the number of apertures per unit length and ω the angular frequency. The diffusion component Z_d of the metal braid is governed by the DC resistance of the metal braid and diffusion of waves through the wall of the cylindrical braid. The second term of (2) is governed by the inductance of magnetic fields through the apertures in the metal braid. The inductance is a local phenomenon. Expressions for this phenomenon are derived by considering the inductance through a single aperture and then superimposing the contributions of all apertures. Hence, the interaction of induced magnetic fields through neighbouring apertures is usually neglected. In general, the inductance comprises three parts: hole inductance, braid inductance and skin inductance. For high frequencies, the inductance dominates over the diffusion component and therefore the transfer impedance will increase linearly with frequency.

The transfer impedance of samples of metal braids can be measured by the so-called line injection method [7]. The measurement set-up is shown in Figure 1. The length of the samples is usually limited to 1 or 2 meters. A picture of samples of which transfer impedance has been measured is shown in Figure 2. These samples have also been discussed in [8]. Since the samples are of finite length, resonances may occur in the measured results if the propagation speed in the injection line is different from the speed in the sample or if the termination impedances of the measurement set-up do not match with the characteristic impedances of the samples.

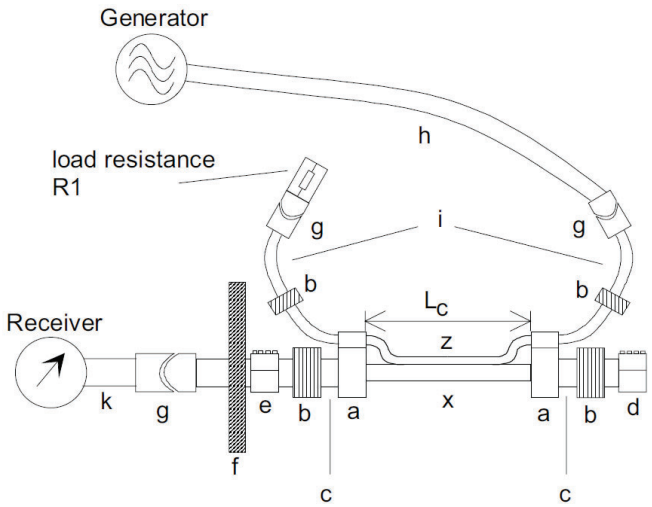

Figure 1 Far-end measurement set-up according to EN 50289-1-6: 2002 [7]

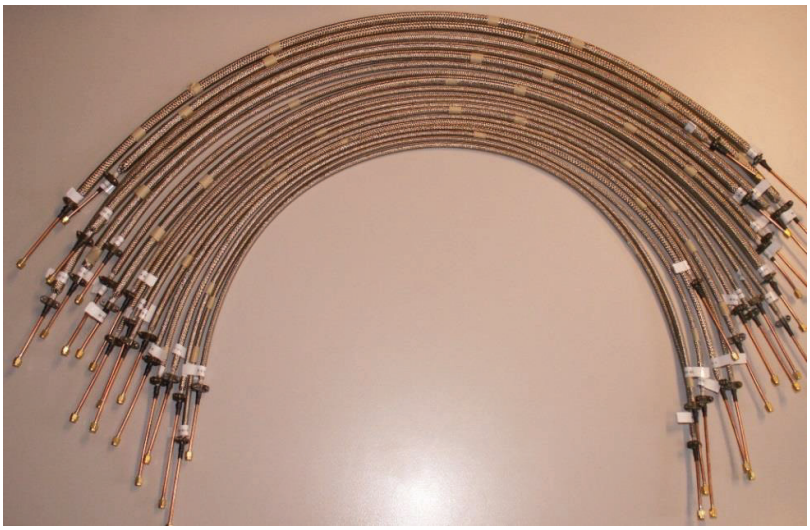

Figure 2 Overview of manufactured samples

Both predicted and measured transfer impedances are sensitive to uncertainties. Possible sources of such uncertainties in the modelling are inaccurate input data (for instance, the exact size of the braid diameter or the wire diameter are not known) and imperfections in the computational model. In the measurements uncertainties can be caused by the mismatch between the characteristic impedance of the samples and the terminations impedances of the measurement set-up. As a consequence, it might be difficult to compare transfer impedance results of analytical models and measurements, specifically in the high-frequency region. However, comparison between simulation and measurement results is necessary for correct validation of the analytical models for transfer impedance. Therefore, in this paper such uncertainties in modelling and measurements are investigated.

The transfer impedances of all metal braids shown in Figure 2 have been measured by the line-injection method [7], and computed by the models as described in [9] and [10]. Results of measurements and calculations have been compared. For some samples good agreement is observed, while for other ones the correlation is poor. The objective of the present paper is to estimate effects of variations of input data on the calculated transfer impedance and to estimate the sensitivity of measured data with respect to mismatch between characteristic impedance and terminations impedances of the measurement set-up.

2. Modelling

2.1 Analytical transfer impedance

In this section the analytical modelling of transfer impedance is concisely described. The metal braids can be characterized by the following six parameters (see also Figure 3):

- Diameter *D* of the braid
- Number of carriers *C* in the braid
- Number of wires *N* in a carrier
- Diameter *d* of a single wire

- Conductivity σ of the wires (dimension S/m)
- Pitch angle (or weave angle) α of the braid

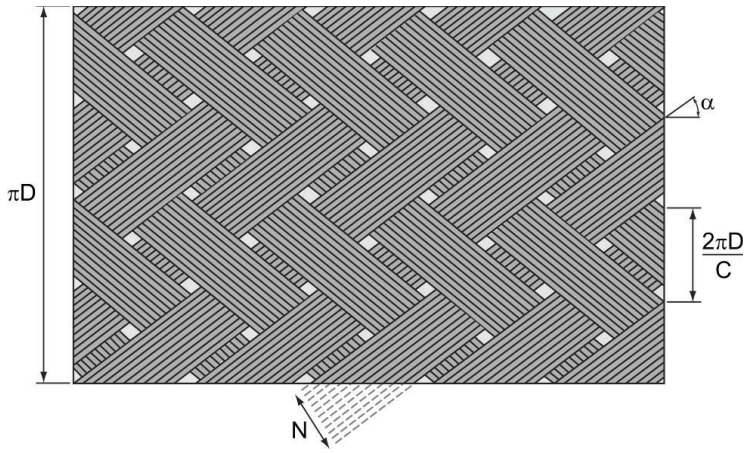

Figure 3 Characteristics of metal braid

Transfer impedance is then calculated by (2), of which the diffusion Z_d is calculated by:

$$Z_d = R_0 \frac{\gamma d}{\sinh \gamma d}, \tag{3}$$

with $\gamma = (1+j)/\delta$, $\delta = \sqrt{2/\omega\mu\sigma}$ and resistance:

$$R_0 = \frac{4}{\pi d^2 NC\sigma \cos(\alpha)}. \tag{4}$$

The hole inductance M_h as part of the inductance in (2) reads:

$$M_h = 0.875 \frac{\mu m}{2\pi^2 D_m^2} e^{-\tau}, \tag{5}$$

with m the magnetic polarizability of a rhombic hole, which follows from:

$$m = S_{rh}^{3/2} \nu, \tag{6}$$

with ν the dimensionless magnetic polarizability of a rhombic hole (see[3]), and S_{rh} is the area of a rhombic hole. Furthermore:

$$\begin{aligned} \tau &= 9.6F \sqrt[3]{F^2 (2-F)^2 d / D_m} \\ D_m &= D_0 + 2d \\ F &= \frac{NCd}{2\pi D_m \cos\alpha}. \end{aligned} \tag{7}$$

The braid inductance M_b is caused by the magnetic flux linkage between the inner and outer braid spindles at the crossovers. Tyni (see [4]) calculates the braid inductance as follows:

$$M_b = -\mu \frac{\hat{h}}{4\pi D_m}(1-\tan^2\alpha), \tag{8}$$

with $\hat{h}$ the average height between the carriers, which by Tyni's model equals:

$$\hat{h} = \frac{2d}{1+b/d}, \tag{9}$$

with b the distance between two adjacent carriers, $b = Nd(1-F)/F$.

The mathematical model described above has been implemented in a Matlab code, which will be referred to in the following sections as BEATRICS [11] (BEtter Analysis of TRansfer Impedance of Cable Shields). In [12] this BEATRICS analytical method was cross-validated against a numerical method which solves the full set of Maxwell's equations in an infinite periodic braided shield with all its wires isolated from each other. The calculated transfer impedances of the analytical and numerical method show good agreement, provided that the average height is calculated according to the distribution of wires between the carriers.

Notice that the magnitude of the braid inductance is directly proportional to the average height $\hat{h}$ between the carriers. In references [6],[13] ,[14] and [15] it has been emphasized that formula (9) overestimates the average height and the contribution of the magnetic flux linkage. In references [14] and [15] more accurate formulas for the calculation of the area between the inner and outer braid spindles have been presented, which yield improved models for the contribution of the braid inductance and better estimates for the average height $\hat{h}$. For braids with high optical coverage the improved model of [15] can be reduced to:

$$M_b = -\mu \frac{\hat{h}}{4\pi D_m}(1-\tan^2\alpha)F\sin 2\alpha. \tag{10}$$

Comparison of (8) and (10) reveals that formula (10) predicts a lower contribution to braid inductance: its magnitude is decreased by a factor $F\sin 2\alpha$. When a new average height is introduced:

$$\overline{h} = \hat{h}F\sin 2\alpha, \tag{11}$$

then formula (10) becomes similar to Tyni's formula (8) where $\hat{h}$ is replaced by $\overline{h}$.

2.2 Modelling of transfer impedance measurement methods

Analytical models of transfer impedance increase linearly with frequency once the inductance terms start to dominate over the diffusion through the braid. These analytical models are independent of the length of the coaxial cable. When measuring transfer impedance, this will always be performed on a test sample of finite length. Therefore, impedance mismatches and differences in propagation

speeds will cause resonances in the measured results. Multiple publications show frequency validity ranges for different measurement techniques [7], [8]. Moreover, [10] shows a way to simulate the measured transfer impedance by multi-conductor transmission line (MTL) modelling. This method includes resonance effects and is quickly adapted to for instance line injection or triaxial methods.

Figure 4 shows an illustration of the test section for the line injection method. The coax under test is separated from an injection wire by a distance *d*. For an MTL model, the shield is chosen as reference and has radius r_S, while the two wires have radii r_1 and r_2. In the exterior of the coax, the current on conductor 1 has its return path via the outside of the shield. In the interior, conductor 2 has its return current on the inside of the shield. Firstly, the multi-conductor transmission line has to be characterised by per-unit-length-parameters and its terminations. The analytical per-unit-length transfer impedance model BEATRICS is also included in these parameters. Thereafter, via MTL simulations the measured transfer impedance can be computed, which can differ from the analytical results in the high frequency area.

2.2.1 Per-unit-length parameters

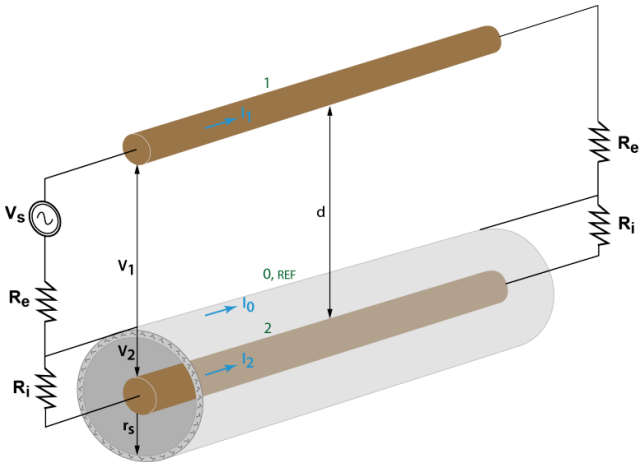

Figure 4: Illustration of a model for the test section of the line injection method

The inductance, capacitance, resistance and conductance matrix contain all geometrical information for the multi-conductor transmission line. Conductance is assumed to be zero, while for the rest expressions are given in this section. Following Paul [16], the inductance and capacitance matrices for the line injection method are given by:

$$\mathbf{L}=\begin{bmatrix} l_{11} & 0 \\ 0 & l_{22} \end{bmatrix}, \qquad \mathbf{C}=\begin{bmatrix} \mu_0\varepsilon_0\varepsilon_{re} & 0 \\ 0 & \mu_0\varepsilon_0\varepsilon_{ri} \end{bmatrix}\mathbf{L}^{-1}, \tag{12}$$

where:

$$l_{11}=\frac{\mu_0}{2\pi}\cosh^{-1}\left(\frac{d^2-r_s^2-r_1^2}{2r_S r_1}\right), \quad l_{22}=\frac{\mu_0}{2\pi}\ln\left(\frac{r_S}{r_2}\right).$$

Here the free space permittivity and permeability are given by ε_0 and μ_0. Homogeneous media with various permittivities can be modelled by changing ε_{ri} and ε_{re}, which correspond to the medium interior and exterior to the coax shield, respectively.

Let the ohmic losses in the two wires be represented by R_{c1} and R_{c2}, while the transfer impedance of the braided shield is given by Z_T. Shield impedances, given by $Z_{sh,i}$ for the interior and $Z_{sh,e}$ for the exterior, are estimated by the shield impedance of a solid copper shield found in [1]. These ohmic losses and shield properties are all contained in the resistance matrix for the line injection method:

$$\mathbf{R} = \begin{bmatrix} R_{c1} & 0 \\ 0 & R_{c2} \end{bmatrix} + \begin{bmatrix} Z_{sh,e} & Z_T \\ Z_T & Z_{sh,i} \end{bmatrix}. \tag{13}$$

2.2.2 Termination circuits

Terminations of the interior and exterior transmission lines are shown in Figure 4. Here R_i and R_e are the resistances at the end of the inner and outer transmission line, respectively. Terminations are equal on both sides of the line, and they are represented in an impedance matrix by:

$$\mathbf{Z}_S = \mathbf{Z}_L = \mathbf{Z} = \begin{bmatrix} R_e & 0 \\ 0 & R_i \end{bmatrix}. \tag{14}$$

In measurements of transfer impedances the termination impedances are matched to the characteristic impedance of the transmission line. Measurement equipment usually has 50 Ω impedance, and thus the interior and exterior transmission lines are designed with the same characteristic impedances. However, in practice it is difficult to create a perfect impedance match. Therefore, the termination resistances will be given by:

$$R_e = \delta\sqrt{l_{11}/c_{11}}, \quad R_i = \beta\sqrt{l_{22}/c_{22}}, \tag{15}$$

where δ and β are equal to 1 if the match is perfect. Mismatched terminations are introduced by choosing one or both of these values unequal to the unit value.

Finally, the excitation of the exterior circuit will be enforced by a voltage source between injection wire and the shield. Therefore, the vectors containing voltage sources at near and far-end side, $\mathbf{V_S}$ and $\mathbf{V_L}$, are equal to:

$$\mathbf{V}_S = \begin{bmatrix} 1 \\ 0 \end{bmatrix}, \ \mathbf{V}_L = \begin{bmatrix} 0 \\ 0 \end{bmatrix}. \tag{16}$$

2.2.3 Computation of measured transfer impedance

The definition of the transmission line properties in the previous section allows simulating the multi-conductor transmission line voltages and currents. Therefore, the following equations need to be solved [16]:

$$\begin{aligned} \mathbf{A}\mathbf{I}_0 &= \left[\Phi_{11} - \mathbf{Z}_L\Phi_{21}\right]\mathbf{V}_S \\ \mathbf{V}_0 &= \mathbf{V}_S - \mathbf{Z}_S\mathbf{I}_0 \\ \mathbf{I}_L &= \Phi_{21}\mathbf{V}_S + \left[\Phi_{22} - \Phi_{21}\mathbf{Z}_S\right]\mathbf{I}_0 \\ \mathbf{V}_L &= \mathbf{Z}_L\mathbf{I}_L, \end{aligned} \tag{17}$$

where:

$$\mathbf{A} = \left[\Phi_{11}\mathbf{Z}_S + \mathbf{Z}_L\Phi_{22} - \Phi_{12} - \mathbf{Z}_L\Phi_{21}\mathbf{Z}_S\right].$$

Here the voltages of the injection wire and the coaxial wire at the near and far-end side are contained in the vectors $\mathbf{V_0}$ and $\mathbf{V_L}$, respectively. Corresponding currents are given by $\mathbf{I_0}$ and $\mathbf{I_L}$. Finally, the $\mathbf{\Phi}$ matrices are the chain parameter matrices. These govern the evolution of voltages and currents along the length of the transmission lines, and carry all per-unit-length information and all propagation effects. Once (17) has been solved for the currents and voltages in all conductors, the transfer impedance can be computed. Measured transfer impedance is derived from the measured voltage, either near or far-end, divided by the injection current:

$$Z_{TN} = 2V_{0,2}/\ell I_{0,1}, \qquad Z_{TF} = 2V_{L,2}/\ell I_{0,1}. \tag{18}$$

Here for example for $V_{0,2}$ the subscripts imply that this is the second entry of the vector $\mathbf{V_0}$.

Taking into account all propagation effects as well as impedance mismatches, the computed transfer impedance from (18) will differ from analytical transfer impedance just as real measurements will. That is, resonances will occur in the high frequency area. Moreover, it is well-known that near and far-end measured transfer impedance will also be different. In section 3.2 the introduced MTL model for the line injection method will be used to investigate sensitivities of measured crosstalk to for instance mismatches and different media interior and exterior to the coax shield.

2.3 Sensitivity coefficient

The sensitivity of transfer impedance with respect to a certain model parameter is a measure for the amount of change in output when the input changes. Sensitivity is therefore always computed for one parameter, while all others are fixed. A normal distribution with given mean μ_x and standard deviation σ_x will be assumed for this random variable X. To obtain sensitivity values the statistical moments of the resulting transfer impedance are required. Therefore, statistical analysis is performed, which leads to N simulation results for N sample values of X. The mean $\hat{\mu}_y$ and standard deviation $\hat{\sigma}_y$ of these simulation results are computed.

Finally, the sensitivity of measured transfer impedance with respect to a model parameter is computed by the ratio of Coefficients of Variation (COV) for input and output. This is defined as:

$$Sensitivity = \frac{COV_{output}}{COV_{input}} = \frac{\hat{\sigma}_y/\hat{\mu}_y}{\sigma_x/\mu_x}. \tag{19}$$

In this way, the sensitivity is a ratio of normalized standard deviations for output (transfer impedance) and input (the uncertain parameter).

3. Theoretical sensitivity analysis

3.1 BEATRICS sensitivity analysis

Sources for uncertainties in analytic transfer impedance models like BEATRICS can be inaccurate input data and imperfections in the computational model. First, we consider uncertainties in the input parameters. A set of 19 samples has been analysed, of which the geometrical parameters are given in Table 1. The conductivity of the metal braids of Table 1 is $\sigma = 4.12\ 10^{-7}$.

Table 1 Overview of geometrical details of metal braids

Sample	D (mm)	d (mm)	N	C	α (°)
1	6	0.202	6	24	25
2	6	0.202	6	24	32
3	6	0.202	5	24	38
4	6	0.202	5	24	41
5	6	0.202	5	24	45
6	6	0.16	7	24	32
7	6	0.16	7	24	35
8	6	0.16	7	24	38
9	6	0.16	6	24	41
10	6	0.16	6	24	45
11	8	0.202	6	32	32
12	8	0.202	5	32	35
13	8	0.202	5	32	38
14	12	0.202	8	32	32
15	12	0.202	8	32	35
16	12	0.202	7	32	41
17	12	0.202	7	32	45
18	12	0.16	7	48	32
19	12	0.16	6	48	35

The sensitivities of the resistance R_0, the hole inductance M_h and the braid inductance M_b were calculated with respect to uncertainties in the input parameters d (thickness of the wires), the diameter D of the braid and the weave angle α. To this end, the values of these parameters were assumed to be normally distributed. The mean values of the three parameters were determined by the prescribed values of the test set of 19 metal braids given in Table 1.

For the thickness d and the braid diameter D the standard deviation s was assumed to be 5%. For the weave angle the standard deviation was taken to be 2%. In total 200 samples for the input parameters were taken from a normal $\mathcal{N}\left(\mu, s^2\right)$ population. By applying the analytical relations (4) , (5) and (8) corresponding outputs for resistance R_0, hole inductance M_h and braid inductance M_b are computed. From this the standard deviations of these output parameters can be obtained. The sensitivity was estimated by the ratio of the calculated standard deviations of the output and input parameters. The resulting sensitivity coefficients of R_0, M_h and M_b with respect to the wire diameter, braid diameter and weave angle are shown in Table 2, averaged for all 19 samples of Table 1.

Table 2 Sensitivity coefficients of DC resistance, hole inductance and braid inductance for errors in wire diameter, shield diameter and weave angle

Sensitivity coefficient	R_0	M_h	M_b
d	2	14.6	3.5
D	0	13.3	3.7
α	0.5	6.1	2.5

These sensitivity coefficients have been used to estimate the total simulation uncertainty due to uncertainty in the input parameters. The simulation uncertainty for DC resistance is given in Table 3. This uncertainty is about twice the uncertainty in the wire diameter. The uncertainty for the hole inductance is shown in Table 4. This value is about 20 times as large as the uncertainty in wire diameter and braid diameter, caused by the high sensitivity for these parameters observed from Table 2.

Table 3 Simulation uncertainty of DC resistance (low frequency Z_t)

Source	Quantity	Value/range	Unit	Uncertainty	Unit	Probability distribution	Standard uncertainty	Unit	Sensitivity coefficient	Uncertainty contribution	Unit
d	wire diameter	2.00E-04	m	5.00	%	normal (k=2)	2.50	%	2.00	5.00	%
sigma	conductivity	4.00E+07	S	5.00	%	normal (k=2)	2.50	%	1.00	2.50	%
alpha	weave angle	4.00E+01	deg	2.00	%	normal (k=2)	1.00	%	0.50	0.50	%
	deltaT / T						combined standard uncertainty (k=1)			5.61	%
							combined expanded uncertainty (k=2)			11.22	%

Table 4 Simulation uncertainty of hole inductance (high frequency Z_t).

Source	Quantity	Value/range	Unit	Uncertainty	Unit	Probability distribution	Standard uncertainty	Unit	Sensitivity coefficient	Uncertainty contribution	Unit
d	wire diameter	2.00E-04	m	5.00	%	normal (k=2)	2.50	%	14.00	35.00	%
D	braid diameter	1.00E-02	m	5.00	%	normal (k=2)	2.50	%	13.00	32.50	%
alpha	weave angle	4.00E+01	deg	2.00	%	normal (k=2)	1.00	%	6.10	6.10	%
	deltaT / T						combined standard uncertainty (k=1)			48.15	%
							combined expanded uncertainty (k=2)			96.30	%

The main imperfection of the BEATRICS computational model is the inaccurate description of the average height $\hat{h}$ between the carriers of a braid. In equation (9) this average height only depends on the wire diameter *d* and the distance *b* between adjacent carriers. The dependence of the transfer impedance on the average height is shown in Figure 5a and Figure 5b for test samples 3 and 11, respectively. The height is varied between *0.1d* and *d*. As expected, the simulations show that the transfer impedances increase with 20 dB per decade with respect to frequency. This increase is compared with the increase of the measured level at intermediate frequencies. For sample 3 the best fit with measurements is obtained for an average height of approximately 0.3*d*. For this sample the average heights calculated by formulas (9) and (11) are 0.8*d* and 0.6*d*, respectively. Hence, for this sample the average height as calculated by (9) or (11) is still overestimated, which results in too high values of the transfer impedance as is shown by Figure 5a. As can be observed from Figure 5b the best fit for sample 11 is obtained for $\hat{h} \approx d$. For this sample the average heights by formulas (9) and (11) are 1.0*d* and 0.8*d*, respectively. Thus, for this sample Tyni's formula (9) predicts the correct

average height, while formula (11) underestimates the average height. Since the braid inductance is directly proportional to the height, the inductance is 10 times as high for *h=d* than for *h=0.1d*. Therefore, it is the large uncertainty in *h* itself causing poor predictions of transfer impedance, and not the sensitivity of the braid inductance for variations in *h*.

The variation in $\hat{h}/d$ across all measured test samples is shown in Figure 6. The values in this figure have been calculated by equations (9) and (11), and by a more advanced expression for the average height that was proposed in [6] and [11]. However, as observed from the best fits in Figure 5a and Figure 5b, the expressions for the average height are still not accurate enough to provide estimates for transfer induction that are in very good agreement with measured results.

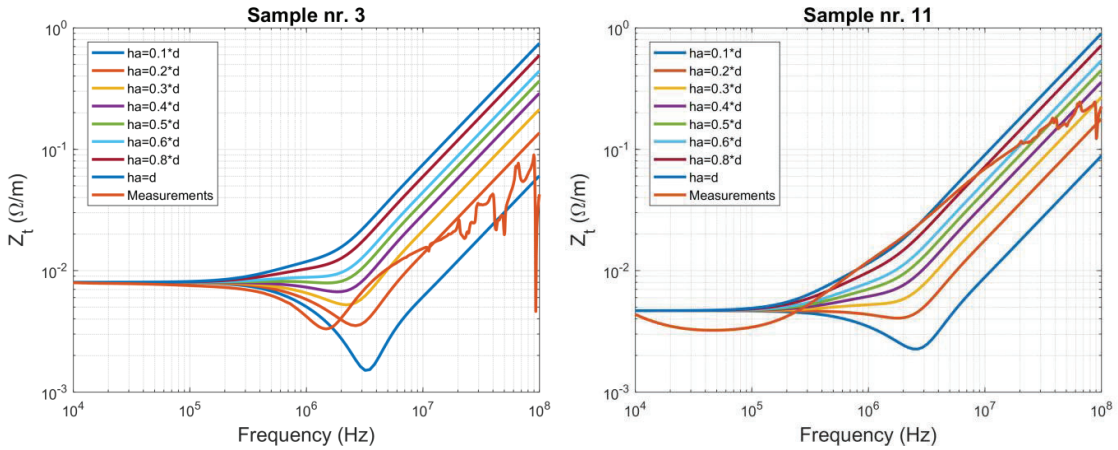

Figure 5 Dependence on average height for a) Transfer impedance of sample 3; b) Transfer impedance of sample 11;

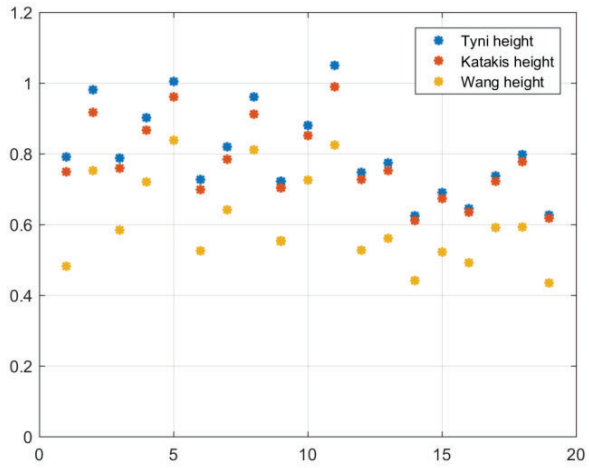

Figure 6 Average height $\hat{h}$ scaled by *d*, as calculated by Eq. (9), Eq. (11) and by Katakis [6] for all samples of Table 1

For samples 3 and 11 the transfer impedance has been computed by the BEATRICS method as presented in section 2.1, by Tyni's method (see [4]) and by the method of Wang [15]. The outcome of the calculations is compared with data of measurements in Figure 7. It can be observed that the computational models predict for sample 3 too much transfer impedance, as could be expected from the above analysis. For sample 11 a fair comparison is observed between computations and

measurements. Moreover, it can be observed that the outcome of BEATRICS and Tyni's method is comparable for such braid samples.

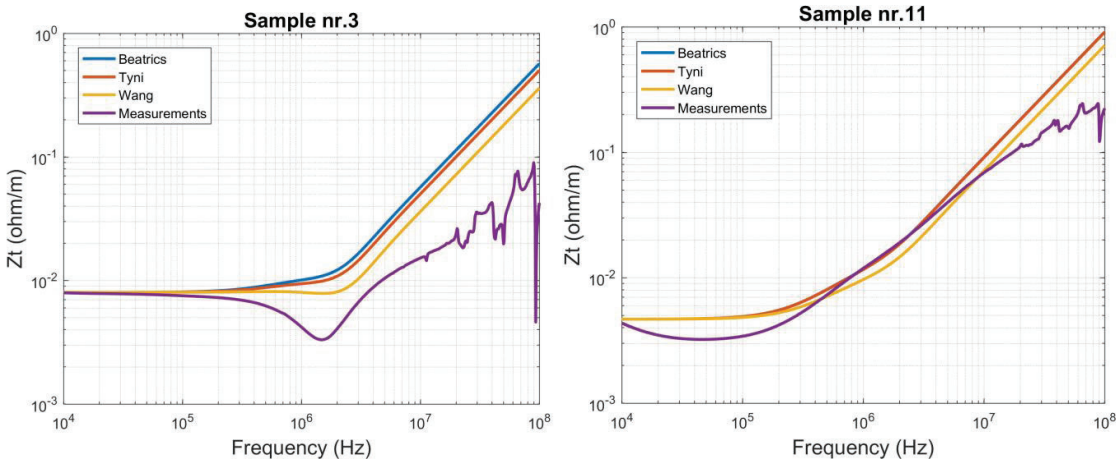

Figure 7: Comparison for two different braid samples between measured transfer impedance, and transfer impedance computed by three different models

From the above analysis it can be concluded that the magnitude of the average height between the carriers strongly determines the value of the transfer impedance at high frequencies. For the design of braids it is therefore recommended to take into account this lack of accuracy. This can be done by considering plus and minus 50 % of the braid inductance, i.e. by multiplying the outcome of (9) by either a factor 0.5 or 1.5. Hence the average height is decreased by 50% and increased by 50%. The results of the transfer impedance calculations are shown in Figure 8. It can be observed that the measured data is more or less in between the bounds of the calculated transfer impedances.

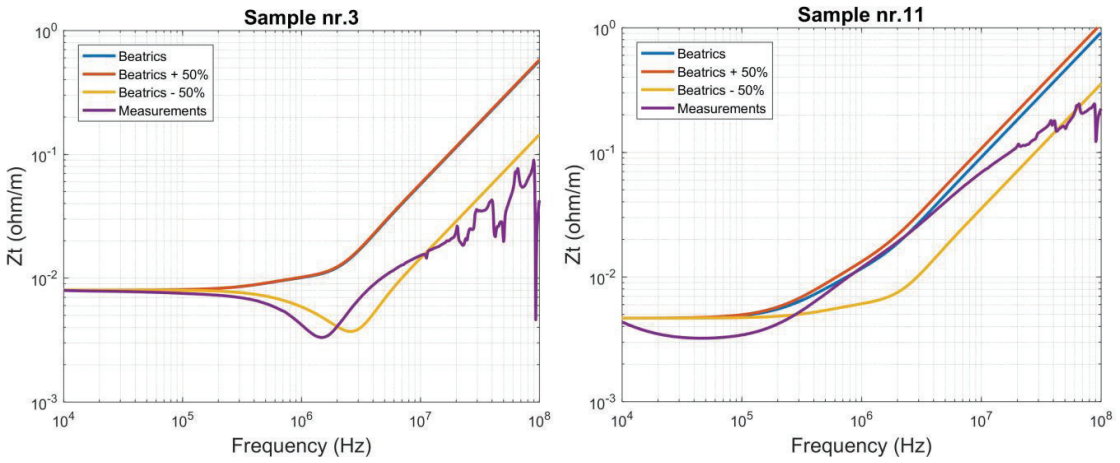

Figure 8: Comparison for two different braid samples between measured transfer impedance, and BEATRICS transfer impedance for three different average heights

The total uncertainty in the braid inductance due to the uncertainty in input parameters is shown in Table 5. The total uncertainty in braid inductance, just as that in hole inductance, is more or less proportional to the uncertainty in the height between the carriers.

Table 5 Simulation uncertainty of braid inductance (high frequency Z_t)

Source	Quantity	Value/range	Unit	Uncertainty	Unit	Probability distribution	Standard uncertainty	Unit	Sensitivity coefficient	Uncertainty contribution	Unit
h	braid distance	1.00E-04	m	50.00	%	normal (k=2)	25.00	%	1.00	25.00	%
D	braid diameter	1.00E-02	m	5.00	%	normal (k=2)	2.50	%	3.70	9.25	%
alpha	weave angle	4.00E+01	deg	2.00	%	normal (k=2)	1.00	%	2.50	2.50	%
	deltaT / T						combined standard uncertainty (k=1)			26.77	%
							combined expanded uncertainty (k=2)			53.55	%

3.2 Sensitivity analysis by MTL simulation

Besides analysing analytical expressions to derive parameter sensitivities, also MTL simulations can be utilized for a sensitivity analysis. Therefore, multiple run simulations are used for the parameter under analysis, from which sensitivity can be determined.

Consider the line injection method of which the MTL model was introduced in section 2.2. The transmission lines interior and exterior to the coax both have a relative permittivity of 2.5. Therefore, the inner coax is filled with a certain dielectric. Moreover, the injection wire is placed against the coax separated by only dielectric insulation of the same material. The radius of the conductor shield equals $r_S = 3\ mm$, while the wire radii are $r_1 = 0.511\ mm$ and $r_2 = 0.8\ mm$. The separation between centre of coax and centre of injection wire equals $d = 4.011\ mm$ and the length of the test section is $\ell = 1\ m$.

Sensitivity is investigated with respect to material properties of inner and outer transmission line, as well as terminations of both lines. Stochastic Reduced Order Models (SROM) are used to efficiently determine the statistics [17]. This is a multiple run algorithm, like Monte Carlo, though the sample values for the random variables are determined as an optimal SROM, by which the number of simulations necessary to obtain converged statistics can be reduced. The optimal SROM is determined by a pattern classification algorithm. For sensitivity analysis only one parameter is varied, which implies that 10 simulations would be sufficient for statistical analysis. In our analysis we have used 16 simulations for the computation of sensitivity. Each simulation leads to a simulated transfer impedance result, and all 16 results are then used to compute the mean and standard deviation (for details, see [17]). From these two quantities, the sensitivity can be computed by using (19).

In the next subsections the sensitivity with respect to termination impedances and permittivities is discussed. Only far-end measured transfer impedance is given, as this is more frequently used than near-end measurements. In all simulations, the input transfer impedance is generated by the BEATRICS model, and is plotted in Figure 9.

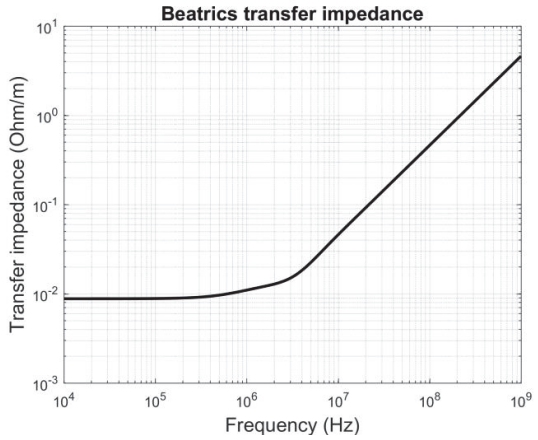

Figure 9: Input transfer impedance for MTL sensitivity analysis

3.2.1 Termination impedances

Firstly, sensitivity with respect to the termination impedances is analysed. Therefore, material properties and all geometrical properties are fixed to the previously given values. The parameters δ and β are both assumed to be normally distributed with mean equal to 1 and standard deviation 0.1.

Figure 10 shows both sensitivity and transfer impedance statistics for variations in β (and δ fixed to 1), which governs impedance mismatches in the internal transmission line. As expected, for low frequencies there is no influence of mismatches to measured transfer impedance. Only for higher frequencies, where the resonances start to occur, there is an effect of impedance mismatch. However, for mismatches with standard deviation of 10% of the characteristic impedance of the interior line, the influence is still small, as is observed from Figure 10b. For $\beta > 1$ the measured transfer impedance will be slightly larger than the analytical value, and for $\beta < 1$ results will be smaller.

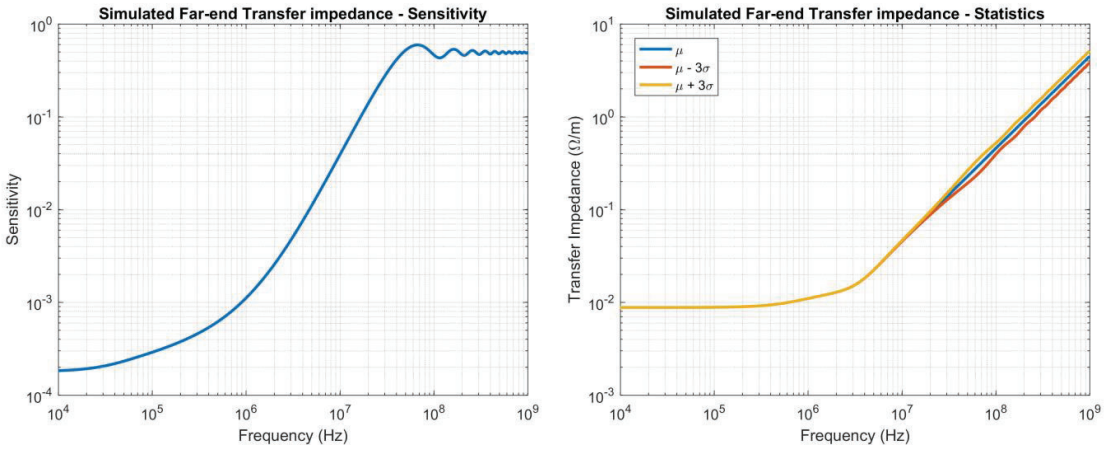

Figure 10: a) (left) Sensitivity with respect to β and b) Transfer impedance statistics for variations in β

Figure 11 shows the sensitivity with respect to the exterior line terminations. That is, the parameter δ has been varied and β is fixed to one to obtain these results. Again, for low frequencies the sensitivity is negligible, but for high frequencies these termination impedances do have influence to

the measured transfer impedance. As opposed to the interior terminations, a deviation from the exterior characteristic impedance causes fluctuations of the measured result around the analytical transfer impedance, while the slope of the trend with respect to frequency is not affected.

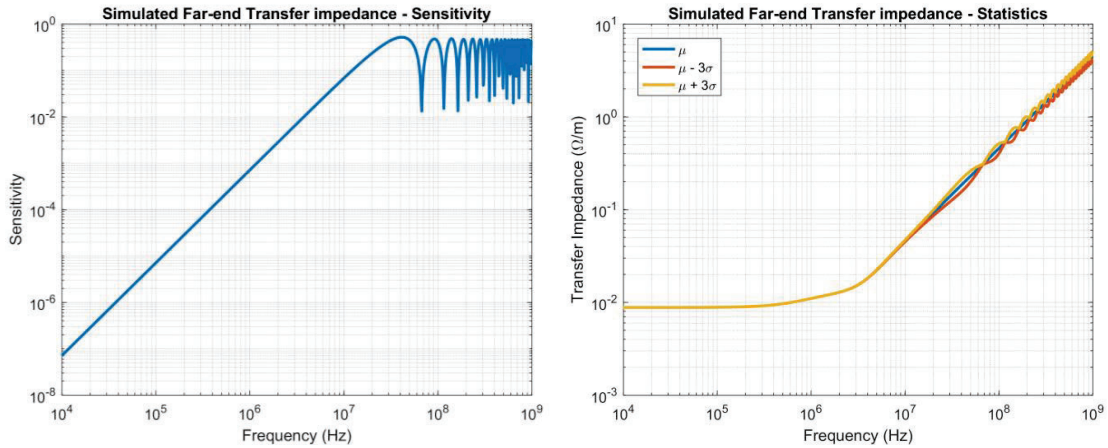

Figure 11: a) (left) Sensitivity with respect to δ and b) Transfer impedance statistics for variations in δ

3.2.2 Permittivities

Secondly, sensitivity with respect to material properties is investigated. Therefore, the termination impedances are now fixed to (15) with $\delta = \beta = 1$. The interior and exterior relative permittivities are varied one at the time. Figure 12 gives sensitivity and statistic results for the case in which the interior material is changed. Clearly, at the point where impedance mismatches and differences in propagation speeds start to have influence the sensitivity is comparable to that in Figure 10. Indeed, changing the permittivity also causes a small impedance mismatch. Though eventually the difference in propagation speeds causes a start of a resonance (see Figure 12b), which makes the increase in sensitivity larger.

Indeed, from theory it is known that the first resonance in measured transfer impedance occurs at [8]:

$$f_r = \frac{1}{\left|v_1^{-1} - v_2^{-1}\right| \ell}. \tag{20}$$

Here v_1 and v_2 are the propagation speeds outside and inside the coaxial cable, respectively. Clearly, when these are equal, there will be no resonance. Moreover, the greater the difference, the earlier a resonance will occur.

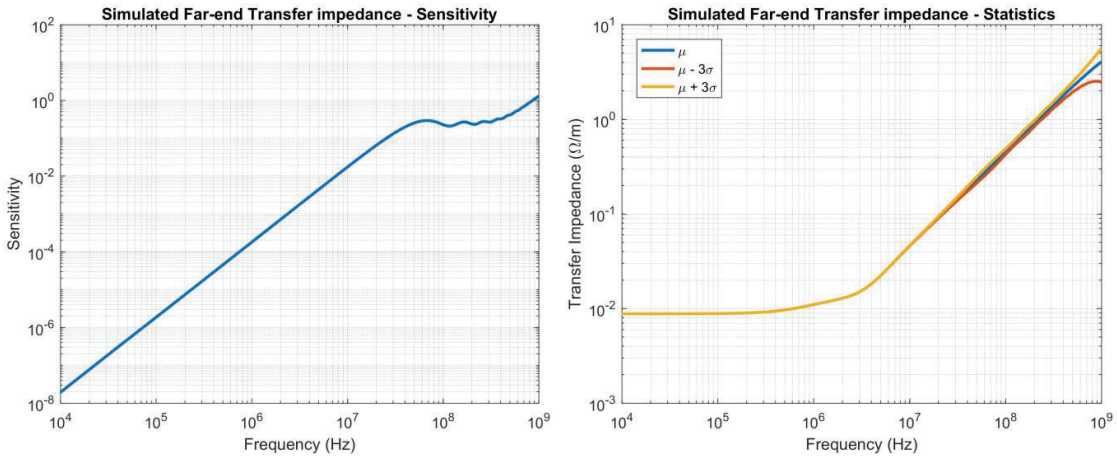

Figure 12: a) (left) Sensitivity with respect to ε_{ri} and b) Transfer impedance statistics for variations in ε_{ri}

The sensitivity with respect to exterior permittivity is similar to that shown in Figure 12. However, sensitivities with respect to permittivities become larger when the initial materials are unequal. In Figure 12 the average permittivities of interior and exterior are equal. Figure 13 shows multiple SROM simulations where ε_{ri} is varied with mean 2.5, while ε_{re} is fixed to 1.5. Clearly, by the mismatch a resonance is present at lower frequency, and varying the interior permittivity changes the position of this resonance. This agrees with (20) and causes the sensitivity to increase to nearly 10 at 1 GHz.

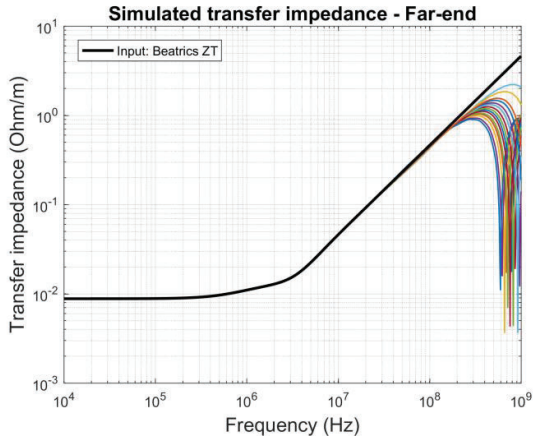

Figure 13: SROM simulations and transfer impedance input (black) for variation in ε_{ri} around 2.5, and $\varepsilon_{re} = 1.5$

Summarizing, Table 6 gives the sensitivity in MTL simulations of measured transfer impedance with respect to the four parameters that were investigated. These values are all for a frequency of 1 GHz. Clearly, the measurement results are more sensitive to a deviation in permittivity of material than they are for a change in termination impedance relative to characteristic impedance.

Table 6: Sensitivities of transfer impedance at a frequency of 1 GHz

Parameter	Transmission line	Sensitivity
Termination impedance	Interior	0.50
	Exterior	0.43
Permittivity	Interior	1.31
	Exterior	1.31

4. Uncertainties in measurements

As mentioned in the previous sections, several methods exist to determine the transfer impedance of metal braids (shields) by measurement: e.g. line injection method or tri-axial method. Each of these methods has its advantages and disadvantages with respect to the frequency range, the accuracy and the practical use. The line-injection method is often used because it can be used up to higher frequencies than the tri-axial method and because it is easier to implement in the case of existing cables (with connectors).

The transfer impedance is a property of the metal braid only. However, in order to measure this transfer impedance, the shield has to be part of a coaxial cable. The metal braid itself has a certain (intended) diameter. In order to avoid any impedance mismatches during the measurement, a coaxial cable has to be made, with the metal braid as shield, which has a characteristic impedance matching that of the measurement equipment (50 Ω). In order to have a 50 Ω characteristic impedance, an inner wire with a proper diameter and an inner dielectric with proper permittivity have to be chosen. After fabrication of the coaxial cable, the characteristic impedance of the cable can be checked by using a vector network analyser.

For the transfer impedance measurement a current has to be injected on the shield of the coaxial cable. The injection circuit that is used for the current injection is an insulated wire close to the shield of the coaxial cable. This insulated wire, together with the shield, constitutes a wire pair with two wires with different diameters. The characteristic impedance of this circuit depends on the wire diameters and on the (average) permittivity of the insulation of the injection wire and the surrounding air. These parameters are selected in a way that also here the characteristic impedance is as close as possible to 50 Ω. This requires a proper selection of the inner conductor radius and the permittivity of the dielectric between shield and inner conductor. If air is used as dielectric small discs should be used to keep the inner conductor at the centre of the sample. This could influence the permittivity slightly.

As mentioned in the sensitivity analysis, it is also important that the permittivity of the injection circuit (the wire pair) and the permittivity of the coaxial cable (with the metal braid) have a similar value. If this is not the case, resonances may appear in the higher frequency range.

The measurement set-up for the far-end is given in Figure 1. The far-end measurement provides reliable results up to a higher frequency than the near-end measurement [7], [8]. A generator is connected to one side of the injection circuit. A measurement receiver is connected to the far-end of the cable under test. The injection circuit and the cable under test are both terminated with a 50 Ω impedance on the side that is not connected to the generator or the measurement receiver. In this case the value of the transfer impedance of the shield under test is determined by the ratio of the voltage measured at the far-end of the coaxial cable (V_m) and the voltage at the near-end of the injection circuit (V_g) [7] (assuming the length of the test section to be 1 m):

$$Z_t = 100\frac{V_m}{V_g}. \tag{21}$$

This (simplified) equation assumes that the capacitive coupling can be neglected because the metal braid has a high optical coverage. For loose single braided cables, capacitive coupling cannot be

neglected. The factor 100 is related to two times the load impedance of the injection circuit (50 Ω). The insertion loss of the measurement cable to the receiver has to be measured and compensated for. Because the shield may not be homogeneous around its circumference, the injection wire is best attached at 4 different positions along the shield (separated by 90^{o}).

From (21) it can be concluded that if the cables are perfectly matched in impedance and the permittivity of both circuits is equal, the uncertainty is mainly determined by the uncertainty in the measurement receiver. If for instance the uncertainty in the amplitude measurement of V_m or V_g is 0.6 dB (1σ), the total uncertainty in the transfer impedance measurement (Zt) is 0.85 dB (1σ) [18]. In the frequency range where resonances due to impedance or permittivity mismatch do not occur yet, the uncertainty of the measurement receiver is the dominant factor in the total uncertainty. In the resonance range, the mismatches may have a larger influence than the uncertainty of the receiver.

5. Conclusions

An analysis of uncertainties in transfer impedance measurements and simulations has been presented. A sensitivity analysis was performed on an analytical model for the prediction of transfer impedance. The results showed that the resistive, low-frequency transfer impedance can be estimated well. The transfer inductance, dominating in the high-frequency region, contains large uncertainties. These are partially caused by uncertainties in the input parameters, of which the average height between the carriers of a braid is most sensitive. Estimations of this height based on the available models are shown to deviate up to a factor 10, which directly affects the estimated hole and braid inductance with similar factors. In practice, reasonable prediction bounds for the high-frequency transfer impedance can be obtained by taking 50% margins on the computed average height.

Moreover, multi-conductor transmission line models for the measurement set-up of transfer impedance have been presented. Results of sensitivity analyses with these models indicate differences between effects of impedance mismatches versus differences in propagation speeds inside and outside the coax. The first causes the measured transfer impedance to deviate slightly from the theoretical transfer impedance. However, the increasing trend caused by transfer inductance is still present, which makes estimation of inductance terms still possible. On the other hand, the differences in propagation speeds cause clearer resonances and higher sensitivities, complicating the estimation of transfer inductance. Therefore, in transfer impedance measurements like the line injection method it would be best to closely match the permittivity inside and outside of the braided shield.

Finally, also the measurement set-up causes uncertainties in transfer impedance measurements. For the measurement of transfer impedance attempts are made to match termination impedances to the characteristic impedance of the coaxial cable. The same holds for equal permittivities inside and outside of the coax. For instance, the insulation material of the injection wire could also be used to fill the coaxial cable. In that case, when pressing the injection wire to the cable shield, the effective permittivity of the outer circuit will be close to that of the interior circuit. In practice however, both the permittivity and the mismatch requirements are not easy to meet exactly, which causes uncertainties in the measurement set-up. Moreover, inhomogeneity of the shield around its circumference implies uncertainties in measured results, as well as uncertainties in the

measurement equipment. The latter are only dominant in the low-frequency results, where resonances are not present.

References

[1] S.A. Schelkunoff, “The electromagnetic theory on coaxial transmission lines and cylindrical shields,” *Bell Systems Techn. Journal 13 (4)*, pp. 532-579, October 1934.

[2] E.F. Vance, Shielding effectiveness of braided-wire shields, Interaction Note 172, Stanford Research Institute, April 1974.

[3] E.F. Vance, Shielding effectiveness of braided-wire shields, *IEEE Transactions on, Electromagnetic Compatibility*, Vol.17, pp. 71-77, 1975.

[4] M. Tyni, The Transfer Impedance of Coaxial Cables with Braided Outer Conductor, FV. Nauk, Inst. Telekomum Akust. Politech Wroclaw, Ser. Konfi, 1975, pp. 410-419.

[5] T. Kley, Optimized Single-Braided Cable Shields, *IEEE Transactions on, Electromagnetic Compatibility*, Vol. 35, pp. 1-9, 1993

[6] J.N. Katakis, Transfer impedance of wire braided coaxial cables at radio and microwave lrequencies. MEng thesis, llniversity of Shefield, February 1983

[7] EN 50289-1-6: 2002 E: “Communication cables - Specifications for test methods Part 1-6: Electrical test methods - Electromagnetic performance,” CENELEC, March 2002.

[8] H. Schippers and J. Verpoorte, "Uncertainties in transfer impedance calculations," *ESA workshop on Aerospace EMC*, Valencia, Spain, 2016.

[9] B. Démoulin, L. Koné, “Shielded cable transfer impedance measurements high frequency range 100 MHz – 1 GHz,” IEEE EMC newsletter (2011), pp. 42-50.

[10] J.H.G.J. Lansink Rotgerink, H. Schippers and J. Verpoorte, “Multi-conductor transmission line modelling of transfer impedance measurement methods,” *Proc. IEEE Int. Symp. Electromagn. Compat.*, Angers, France, 2017.

[11] H. Schippers and J. Verpoorte, "Hole inductance in braided cable shields," *Proc. IEEE Int. Symp. Electromagn. Compat.*, Dresden, Germany, 2015.

[12] R. Otin, J. Verpoorte, H. Schippers and R. Isanta, "A finite element tool for the electrocmagnetic analysis of braided cable shields," *Computer physics communications,* vol. 191, pp. 209-220, 2015.

[13] F.A. Benson, F.A.; P.A. Cudd,; J.M Tealby; Leakage from Coaxial Cables, *IEE Proceedings A*, Vol. 139, pp. 285-303, 1992.

[14] S. Sali, An improved model for the transfer impedance calculations of braided coaxial cables, *IEEE Trans. on Electromagnetic Compatibility*, Vol. 33, pp. 139-143, 1991.

[15] Wang Xiaoling, Liu Chao, Ding Hao, Wang Lixin, “An Improved Model for the Transfer Impedance Calculations of Braided Coaxial Cables,” *IEEE 7th Int. Power Electronics and Motion Control Conference - ECCE Asia*, Harbin, China, 2012, pp. 1078-1081.

[16] C.R. Paul, “Analysis of multiconductor transmission lines,” New York, John Wiley & Sons, 1994.

[17] Z. Fei, Y. Huang, J. Zhou and Q. Xu, “Uncertainty quantification of crosstalk using stochastic reduced order models,” IEEE Trans. Electromagn. Compat., vol. 59, no. 1, Feb. 2017.

[18] Lab34, “The expression of uncertainty in EMC testing,” UKAS, Edition 1, 2002.